REPORT DOCUMENTATION PAGE

Form Approved
OMB No. 074-0188

1. AGENCY USE ONLY (Leave blank)	2. REPORT DATE	3. REPORT TYPE AND DATES COVERED
	October 94 - September 95	Annual Report, October 1994 - September 1995

4. TITLE AND SUBTITLE
Advanced Polyelectrolyte-Modified Zinc Phosphate Coatings

5. FUNDING NUMBERS
DOE
Contract No. DE-AC02-76CH00016

US Tank Automotive Command
Contract No. D005/F074

6. AUTHOR(S)
T. Sugama, N. Carciello and C.I. Handsy

7. PERFORMING ORGANIZATION NAME(S) AND ADDRESS(ES)

Energy Efficiency and Conservation Division, Department of Applied Science, Brookhaven National Laboratory, Associated Universities, Inc. Upton, Long Island, NY 11973

U.S. Tank Automotive Command, Warren, MI 48090-9055

8. PERFORMING ORGANIZATION REPORT NUMBER
N/A

9. SPONSORING / MONITORING AGENCY NAME(S) AND ADDRESS(ES)
SERDP
901 North Stuart St. Suite 303
Arlington, VA 22203

10. SPONSORING / MONITORING AGENCY REPORT NUMBER
N/A

11. SUPPLEMENTARY NOTES
This work was performed under the auspices of the U.S. DOE, Washington, D.C. under Contract No. DE-AC02-76CH00016, and supported by the U.S. Tank Automotive Command, under Contract No. D005/F074. The United States Government has a royalty-free license throughout the world in all copyrightable material contained herein. All other rights are reserved by the copyright owner..

12a. DISTRIBUTION / AVAILABILITY STATEMENT
Approved for public release: distribution is unlimited

12b. DISTRIBUTION CODE
A

13. ABSTRACT ***(Maximum 200 Words)***

The aim of our work was to develop polyelectrolyte-modified zinc phosphate conversion coatings to protect cold-rolled steels against corrosion. Accordingly, we formulated environmentally acceptable material systems for the zinc phosphating make-up solution, and developed the process technology to meet this purpose. The basic formulation consisted of 5 wt% $Zn_3(PO_4)_2 \bullet 2H_2O$, 10 wt% (86 % H_3PO_4) and 85 % water; appropriate amounts of the $Mn(NO_3)_2 \bullet 6H_2O$ and $FeSO_4 \bullet 7H_2O$ as additives were incorporated into the basic formulation. The former had two important functions; one was to create a large number of nucleate sites of embryonic Zn•Ph crystals on the steel surfaces, and the other was to act as an inhibitors of corrosion. The latter additive served to rapidly promote the rate of crystal growth. Poly (acrylic acid), [p(AA)], which is one of the anionic polyelectrolyte species, was employed as the replacement for the conventional Cr-related compounds which are commonly used in the rinsing solutions of Zn•Ph coatings. The p(AA)-rinsed Zn•Ph coatings not only displayed an excellent salt-spray resistance of > 1000 hrs, but also contributed to the strong electrochemical affinity with the electro-deposited polymer topcoatings.

14. SUBJECT TERMS
polyelectrolyte-modified zinc phosphate conversion coatings, SERDP

15. NUMBER OF PAGES
34

16. PRICE CODE
N/A

17. SECURITY CLASSIFICATION OF REPORT	18. SECURITY CLASSIFICATION OF THIS PAGE	19. SECURITY CLASSIFICATION OF ABSTRACT	20. LIMITATION OF ABSTRACT
unclass	unclass	unclass	UL

ıama, T., N. Carciello, and C.I. Handsy. *"Advanced Polyelectrolyte Modified Zinc Phosphate Coatings."* Annual Report, prepared for U.S. Tank Automotive Command, Warren, MI by Brookhaven National Laboratory, Long Island, NY, DOE Contract Number DE-AC02-76CH00016, October 1994 - September 1995.

263 - 1995

ADVANCED POLYELECTROLYTE-MODIFIED ZINC PHOSPHATE COATINGS

FINAL - FY-95

Phase I.

Annual Report
(October 1994 - September 1995)

by
T. Sugama, N. Carciello and C.I. Handsy*

Energy Efficiency and Conservation Division
Department of Applied Science
Brookhaven National Laboratory
Associated Universities, INC.
Upton, Long Island, NY 11973

* AMSTA-~~TMC~~ TRE / MATLS
U.S. Tank Automotive Command
Warren, MI 48090-9055

This work was performed under the auspices of the U.S. Department of Energy, Washington, D.C. under Contract No. DE-AC02-76CH00016, and supported by the U.S. Tank Automotive Command, under Contract No. D005/F074.

ABSTRACT

The aim of our work was to develop polyelectrolyte-modified zinc phosphate conversion coatings to protect cold-rolled steels against corrosion. Accordingly, we formulated environmentally acceptable material systems for the zinc phosphating make-up solution, and developed the process technology to meet this purpose. The basic formulation consisted of 5 wt% $Zn_3(PO_4)_2 \cdot 2H_2O$, 10 wt% (86 % H_3PO_4) and 85 % water; appropriate amounts of the $Mn(NO_3)_2 \cdot 6H_2O$ and $FeSO_4 \cdot 7H_2O$ as additives were incorporated into the basic formulation. The former had two important functions; one was to create a large number of nucleate sites of embryonic Zn·Ph crystals on the steel surfaces, and the other was to act as an inhibitors of corrosion. The latter additive served to rapidly promote the rate of crystal growth. Poly(acrylic acid), [p(AA)], which is one of the anionic polyelectrolyte species, was employed as the replacement for the conventional Cr-related compounds which are commonly used in the rinsing solutions of Zn·Ph coatings. The p(AA)-rinsed Zn·Ph coatings not only displayed an excellent salt-spray resistance of > 1000 hrs, but also contributed to the strong electrochemical affinity with the electro-deposited polymer topcoatings.

1. Introduction

In earlier work at Brookhaven National Laboratory (BNL) performed under U.S. Army Research Office (ARO) and U.S. Tank Automotive Command (TACOM) sponsorships, we studied the characteristics of polyelectrolyte-incorporated zinc phosphate conversion coatings deposited onto cold-rolled steel (CRS) surfaces. The coatings were deposited by immersing the CRS substrates into a phosphating solution bath consisting of four components; polyelectrolyte macromolecule, zinc orthophosphate [$Zn_3(PO_4)_2 \cdot 2H_2O$], phosphoric acid (H_3PO_4), cobalt or nickel nitrate hydrates, and water at 80°C. We also were interested in their ability to protect the CRS from corrosion [1-6]. The specific manner in which these components were converted into zinc phosphate (Zn·Ph) crystals to entirely cover all the CRS surfaces was as follows; crystalline $Zn_3(PO_4)_2 \cdot 2H_2O$ powder was dissolved into the H_3PO_4 solution through a dissolution-recrystallization conversion process, which implies that the Zn·Ph compound deposited on the CRS surfaces is the essentially same $Zn_3(PO_4)_2 \cdot 2H_2O$ as that used in the converting solution. The Co or Ni nitrates were used as cathodic reaction activators to create numerous nucleate sites of embryonic Zn·Ph crystals on the CRS surfaces. Because the presence of many such sites ensures the formation of dense, packed Zn·Ph crystal coatings, it is very important that a large number of them are generated.

From the standpoint of the desired morphological features of Zn·Ph crystals, we identified that one ideal feature in providing a good protection was an array of tightly packed, fine grained Zn·Ph. There are the two potential techniques for producing small crystals; one is to incorporate foreign elements with different atomic radii into the crystal lattice, and the other was to suppress crystal growth by adding a polyelectrolyte macromolecule having a carboxylic and sulfonic pendant groups. Such suppression was due primarily to the chemisorption of the polyelectrolyte either on newly precipitated crystal embryos, or on growth sites during the primary crystallization processes. For the latter method, we used poly(acrylic acid), p(AA) as the polyelectrolyte, and its proper amount was incorporated into the phosphating solutions. The Zn·Ph coatings derived from this polyelectrolyte-incorporated zinc phosphating solution not only contributed significantly to inhibiting the corrosion of CRS, but also showed excellent adherence to the polymeric topcoats because of the presence of functional p(AA) at the outermost surface sites of Zn·Ph layers.

However, the major problem encountered in using this process technology was

the fact that when the ratio of the surface area of substrates to the volume of phosphating solution was very low, it was very difficult to prepare a void-free continuous Zn·Ph layer in a short immersion time; any voids that were present promoted the corrosion of CRS. Considering that ferrous (Fe^{+}) ions dissociated electrochemically from the CRS surfaces at the CRS-phosphating solution interfaces serve to promote the rate of conversion of Zn·Ph, the reason for a poor conversion was due mainly to a lack of Fe^{2+} ions in the phosphating bath. In other words, the concentration of Fe^{2+} ions liberated from CRS, when the ratio of CRS surface area to solution volume was low, was not enough to accelerate the precipitation of Zn·Ph crystals. To solve this problem, ion(II)sulfate heptahydrate ($FeSO_4 \cdot 7H_2O$) was dissolved in the phosphating bath to generate more Fe^{2+} before immersing the CRS test panels into the make-up solution. However, when the concentration of Fe^{2+} ions reached a certain higher level, we encountered another problem; namely, the p(AA) polyelectrolyte favorably reacted with the Fe^{2+} ions. Such an ionic reaction caused the precipitation of a large amount of Fe-complexed p(AA) compounds, implying that the phosphating solutions no longer had the ability to deposit Zn·Ph on the metals. This finding gave us the information that the p(AA) should not be incorporated into the Fe^{2+} ion-enriched phosphating solution to prevent the undesirable polyelectrolyte complex compound formed by uptake of Fe^{2+} ions being precipitated. As described in our previous papers [2], one of the major characteristics of p(AA) in providing corrosion protection was its strong chemisorption on the Zn·Ph layers. Thus, the elimination of p(AA) from the Zn·Ph coating processes is very regrettable. Our idea in applying p(AA) in this process was to use it as the replacing material for the Cr-related compounds (corrosion inhibitors) which are frequently added to the rinsing solution for the Zn·Ph layers because Cr compounds are environmentally unacceptable.

On the other hand, when the cleaning solution of CRS surfaces before treating it with phosphating solution was considered, the use of strong alkali cleaning solutions frequently resulted in the formation of undesirable oxide or hydroxide layers on the substrate topsurface. These layers act to inhibit the creation of local cathodic reaction sites at which the insoluble embryonic Zn·Ph crystals form. Even though an oxide remover was used, it was found to be very difficult to completely remove these layers from the underlying metal. As expected, the presence of an abundance oxide or hydroxide layer at the

topsurfaces of CRS resulted in a poor coverage of Zn·Ph layers over the substrate.

Due to the environmental issues of the Zn·Ph conversion coatings, considerable attention was paid to the Cr-, Ni-, and Co-containing chemical reagents used as cathodic reaction activators to develop embryonic crystal nucleate sites and also as corrosion inhibitors. These transition metals are known to be environmentally hazardous. Thus, processes are needed in which they can be replaced by environmentally benign metal-containing compounds.

The objective of Phases I of this program, which was scheduled to be accomplished in the contract period of October, 1994 through September, 1995, was to gain the technical information on the following five topics; 1) the effect of additional Fe^{2+} ions on increasing the rate of conversion, 2) the replacement with other metal nitrate compounds of the environmentally hazardous Co-, Ni-, and Cr-nitrates, 3) the substitution of environmentally safe polyelectrolyte for the conventional chrome-based compounds in the rinsing process, 4) the extent of affinity of polyelectrolyte-rinsed Zn·Ph surfaces to electrically deposited polymeric topcoatings, and 5) the use of biodegradable enzymatic cleaning solutions as a method to inhibit the formation of oxides or hydroxides on the CRS surfaces. Unfortunately, the last topic was not completed in this FY; we are continuing work to finalize our results. All the data obtained, excepting the last problem were correlated directly with the results from the corrosion-related experiments, such as potentiodynamic polarization measurement and electrochemical impedance spectroscopy, and salt-spray resistance. Based upon the knowledge acquired, our final attempt to reach the goal of this program was to design an optimum formulation for the zinc phosphating solution for the cold-rolled steels, and to propose a new process technology suitable for this formulation.

2. Experimental Details

2.1 Materials

The metal substrate used was an AES 1008 cold-rolled steel test panel (4 in. x 6 in.) supplied by Advanced Coating Technologies, INC. These test panels, which already were cleaned by supplier were employed in all experiments. The basic formulation for the zinc phosphating solution was 5.0 wt% zinc orthophosphate [$Zn_3(PO_4)_2 \cdot 2H_2O$, Johnson Matthey Co.], 10 wt% phosphoric acid [86

% H_3PO_4, Barker Chemical Co.], and 85 wt% deionized (D.I.) water. It was modified by incorporating metal nitrate hydrate compounds [$M(NO_3)_x \cdot yH_2O$, where M is Co, Mg, Ca, Fe, Cu, Mn, or Al, x is 2 or 3, and y is 4, 5, or 9] and iron (II) sulfate heptahydrate ($FeSO_4 \cdot 7H_2O$), supplied by Aldrich Chemical Company. The former compounds were used as cathodic reaction activators for creating the crystal nucleate sites, and the amount added was 1 % by weight of the total zinc phosphating solution. The $FeSO_4 \cdot 7H_2O$ was employed to incorporate a certain number of ferrous (Fe^{2+}) ions which serve as an accelerator of crystal growth into the zinc phosphating solution. The amount of this reagent ranged from 1 to 3 % by weight of the phosphating solution. The water-soluble polyelectrolyte polymer chosen as the rinsing material of Zn·Ph surfaces was poly(acrylic acid) [p(AA), Rohm and Haas Company] as concentrations ranging from 1.3 to 5.0 wt% in aqueous solution. The average molecular weight of the p(AA) was ≈ 60,000. The Zn·Ph conversion coatings were prepared in accordance with the following sequence. As the first step, a certain amount of $FeSO_4 \cdot 7H_2O$ was dissolved in the phosphating solution to generate free Fe^{2+} ions. Second, the surface-cleaned test panels were immersed for 30 min in the Fe^{2+}-containing phosphating solution at 80°C, the panels withdrawn from the bath, and then rinsed with water to wash off any acid contaminants from the Zn·Ph surfaces. Next, the rinsed Zn·Ph panels were dipped for a few seconds into the p(AA)-rinsing solution. Finally, the p(AA)-wetted Zn·Ph panels were dried in an oven at temperatures up to 150°C for 20 min to fabricate the solid p(AA) thin films over the Zn·Ph surfaces, and to fill voids and fissures in the Zn·Ph layers.

In preparing the polymeric topcoating, all the p(AA)-treated Zn·Ph panels were coated with the polyurethane-modified epoxy copolymer (POWERCRON 648) by electrodeposition technology at PPG industries, Inc. The polymeric topcoat was cured in a gas oven at ≈ 177°C for 30 min.

2.2 Measurements

The concentration of Fe^{2+} ions in the phosphating solution was determined by titration in the following way; 10 ml of the solution was placed in a clear beaker, and then 10 to 15 drops of 50 % H_2SO_4 were added to the sample. Next, the H_2SO_4-containing sample was titrated by adding 0.042 N $KMnO_4$ solution until its color changed from a colorless transparent liquid to pink. Subsequently, the concentration of Fe^{2+} ions as percentage was obtained by multiplying by 0.023 the

total amount (ml) of 0.042 N $KMnO_4$ used.

The microtopography and chemical composition of the Zn·Ph coating surfaces was investigated using AMS 10 nm scanning electron microcopy (SEM) coupled with TN-2000 energy-dispersion x-ray spectrometry (EDX).

DC potentiodynamic polarization measurement for data on the rate of corrosion was made with an EG&G Princeton Applied Research Model 362-1 Corrosion Measurement System. The electrolyte was a 0.5 M sodium chloride solution, made from distilled water and reagent grade salt. The specimen was mounted in a holder, and then inserted into a EG&G Model K47 electrochemical cell. The tests were conducted in an aerated 0.5 M NaCl solution at 25°C, on an exposed surface area of 1.0 cm^2. The polarization curves containing the cathodic and anodic regions were measured at a scan rate of 0.5 mv/sec in the corrosion potential range of -1.0 to -0.4 volts. AC electrochemical impedance spectroscopy (EIS) was used to evaluate the ability of coating films to protect the steel from corrosion. The specimens were mounted in a holder, and then inserted into an electrochemical cell. Computer programs were prepared to calculate theoretical impedance spectra and to analyze the experimental data. Specimens with a surface area of 13 cm^2 were exposed to an aerated 0.5 N NaCl electrolyte at 25°C, and single-sine technology with an input AC voltage of 10 mV (rms) was used over a frequency range of 10 KHz to 1 mHz. The lower frequency limit was chosen because of time limitations. To estimate the protective performance of coatings, the pore resistance, R_{po} was determined from the plateau in Bode-plot scans (impedance, ohm-cm^2 vs. frequency, Hz) that occurred at low frequency regions. The salt-spray tests of Zn·Ph-coated panels were carried out in accordance with ASTM B 117, using a 5 % NaCl solution at 35°C.

3. Results and Discussion

3.1 Ferrous (Fe^{2+}) Ions in Phosphating Solution

To investigate the effect of incorporating Fe^{2+} ions dissociated from $FeSO_4 \cdot 7H_2O$ in the phosphating solution on the effectiveness of the Zn·Ph layers in protecting the metal against corrosion, we undertook two important researches; one was to observe the Zn·Ph-coated panel surfaces by an optical microscopy to assess the extent of coverage of panel surfaces by Zn·Ph layers as a function of concentration of Fe^{2+} ions; the other was to test the salt-spray resistance of

Zn·Ph panels treated with phosphating solutions containing various concentrations of Fe^{2+} ions, ranging from 0.0 to 1.0 %. In this study, a 1.0 wt% $Co(NO_3)_2 \cdot 6H_2O$-modified zinc phosphating solution was used. The results from these specimens are shown in Table 1. As seen, these properties depended primarily on the changes in concentration of free Fe^{2+} ions; namely, an increase in its concentration led to a more extensive coverage by Zn·Ph layers and an improvement in salt-spray resistance. Fe^{2+} ions at concentration of at least 0.52 % seem to be needed to obtain a reasonable coverage of the panel's surfaces by Zn·Ph layers without generating visually identical voids, and reflecting a salt-spray resistance of 72 hrs. Increasing the Fe^{2+} concentrations to 0.86 % resulted in a further improved resistance. It is clear that Fe^{2+} ions of > 0.52 % must be incorporated into an phosphating solution to ensure that a continuous, uniform Zn·Ph layer is deposited onto the panel surfaces.

3.2 Cathodic Reaction Activators and Corrosion Inhibitors

Emphasis in this topic was directed towards three subjects: 1) investigating the activity of nitrate in the metal nitrate compounds used as cathodic reaction activators to develop embryonic crystal nucleate sites on the metal surfaces, 2) exploring the morphological and topographical features, and inspecting the chemical components of the surfaces of the Zn·Ph layer derived from various metal nitrates-modified phosphating solutions, and 3) comparing the effects of different metal ions liberated from the nitrate compounds in the phosphating solution on inhibiting the corrosion. Because an assignment of cathodic reaction activators creates numerous reaction sites which serve in providing the formation of dense, packed, and continuous Zn·Ph crystal layers, the study on the first subject was focused upon a comparison of the rates of corrosion for the Zn·Ph-coated panels prepared in the metal nitrate compound-modified and unmodified phosphating solutions. In this study, $Co(NO_3)_2 \cdot 6H_2O$ was used as the metal nitrate compound. Table 2 shows the results from the salt-spray resistance tests for the modified and unmodified Zn·Ph panels as a function of concentration of Fe^{2+} ions. Although the salt-spray resistance was improved by incorporating a high concentration of Fe^{2+} ions, its resistance of Zn·Ph panels derived from the unmodified solution containing 1.10 % Fe ions was only 24 hrs. Examination of this panel (not shown) by optical microscopy revealed the presence of a large number of voids in the Zn·Ph layers. The formation of such a

discontinuous Zn·Ph layer strongly suggested that the crystal nucleate sites of the surfaces of panels treated with the nitrate-free solution were far fewer. In contrast, Co nitrate-modified Zn·Ph panels prepared with 1.0 % Fe ions displayed a resistance of 82 hrs, and no voids were observed. Thus, the Co nitrate compound appears to create many crystal nucleate sites on the panel surfaces, thereby forming a void-free continuous Zn·Ph layer. However, there is no evidence whether the cathodic reaction that created such sites was promoted by the ionic nitrate species or by metal ions dissociated from the metal nitrate compounds in the phosphating solution. To replay for this question, we explored the morphological and topographical features of Zn·Ph coatings derived from the Ca-, Cu-, Al-, Fe-, Co-, and Mn- nitrate compounds-modified phosphating solutions by scanning electron microscopy (SEM). Also, the surface elemental components of these coatings were detected using the energy-dispersive x-ray spectrometry (EDX) coupled with SEM. The SEM image of $Ca(NO_3)_2 \cdot 4H_2O$-modified Zn·Ph coating surfaces is characterized by microstructure features which indicate an interlocking topography of typical rectangular and plate-shape Zn·Ph crystals precipitated on the test panel (see Figure 1, top). No voids were observed in the SEM micrographs, implying that the panel surfaces were completely covered by Zn·Ph layers. The elemental distributions which exist at the depths of several microns from the Zn·Ph surface can be surveyed using an EDX spectrum; this coating showed an intensive signal of P and Zn as the major elemental components, together with a moderately intense Fe and O signal, suggesting that the Zn·Ph layers contain a certain amount of Fe. The detected Au come from the sputtered gold film. However, there was no signal from Ca, revealing that Ca ions released from the nitrate compound are not introduced into the crystal. Although the size of crystals is somewhat bigger than those from the Ca nitrate-modified Zn·Ph system, a similar morphology was seen on the $Cu(NO_3)_2 \cdot 3H_2O$-modified Zn·Ph surfaces (Figure 1, bottom). The EDX spectrum for this Zn·Ph system revealed features resembling those of the Ca system. Again, no Cu element was detected. By comparison, the crystal morphology resulting from including $Al(NO_3)_3 \cdot 9H_2O$ in the phosphating solution was much different. In this case (see Figure 2, top), the image showed the precipitation of a lamella-like cluster crystal on the substrate. As is evident from EDX spectrum of the area denoted as the site "a", this cluster was identified as being the Fe-containing Zn·Ph compounds. The image also showed that the growth of cluster-type crystals seems to result in a poor coverage of the

substrate surfaces by the Zn·Ph layer because of the presence of some voids in the layer. In fact, EDX inspection of site "b" showed a dominant Fe signal, corresponding to the underlaying steel panel. We believed that this discontinuous layer of cluster Zn·Ph crystals caused the increase in the rate of corrosion. By comparison, the microstructure of the $Fe(NO_3)_3 \cdot 9H_2O$ system-derived conversion coating (see Figure 2, bottom) revealed a dense morphology of wide plate crystals coexisting with rectangular-type crystals, which is quite similar to those of the Ca- and Cu-nitrate systems. Furthermore, the EDX spectral feature of this crystal was the same as those of these nitrate systems. The SEM-EDX results from the $Co(NO_3)_2 \cdot 6H_2O$- and $Mn(NO_3)_2 \cdot 6H_2O$-derived Zn·Ph coatings are given in Figure 3, top and bottom, respectively. However, even though these crystalline coatings exhibited a similar microtexture to those of the Ca-, Cu-, and Fe-nitrate systems, some features of the EDX spectra for these crystals were markedly different; the following three being the major one: the first was the presence of Co and Mn signals in the spectra, reflecting the introduction of Co and Mn elements into the crystal layers; the second was the fact that a secondary Zn line at 1009 eV become the most intensive peak; and the third one was the relatively low count of the Fe signal peak. It is very interested to note that the phosphating solutions modified with Co- and Mn- nitrates were attributable to the precipitation of Zn-rich Zn·Ph layers containing a certain content of Co and Mn elements, and a low content of Fe. The results also strongly verified that the creation of cathodic reaction sites on the metal panel's surfaces depends on the ionic nitrate species dissociated from the metal nitrate compounds in the phosphating solution, but is independent of the metal ions. Hence, void-free continuous layers of Zn·Ph over the panels can be prepared by using phosphating solutions modified with any of metal nitrate compounds, excepting the Al nitrate.

Next, our attention focussed on investigating the role of metal ions liberated from the nitrate compounds in preventing the corrosion of the panels. The various metal nitrate-derived Zn·Ph coatings were examined using the AC electrochemical impedance spectroscopy (EIS) and DC potentiodynamic polarization measurement. All the data then were correlated to the results from the salt-spray resistance tests for these coatings. Figure 4 compares the Bode-plot features (the absolute value of impedance, $|Z|$, ohm-cm^2 vs. frequency, Hz) of the bare steel panel and $Mn(NO_3)_2 \cdot 6H_2O$-modified Zn·Ph/steel panels. Our particular attention in the overall impedance curve was given to the impedance value of the

element $|Z|$, which can be determined from the plateau in the Bode plot occurring at sufficiently low frequencies [7]. The impedance of the uncoated panel substrate was $\approx 1.8 \times 10^2$ ohm-cm^2 at a frequency of 0.5 Hz. Once the panel surfaces were coated with the Zn·Ph, the impedance in the terms of the pore resistance, R_{po}, of the coatings increased two-fold over that of the substrate. The R_{po} values reflect the magnitude of ionic conductivity generated by the electrolyte passing through the coating layers; namely, a high value of R_{po} corresponds to a low degree of penetration of electrolyte into the coating film [8]. Table 3 gives the impedance values of the Zn·Ph coatings derived from the phosphating solutions modified with Ca-, Mg-, Cu-, Fe-, Al-, Co-, and Mn-nitrate compounds. As seen, the $|Z|$ value for all the coatings, except for Al-nitrate, ranged from 4.0×10^2 to 4.8×10^2. In other words, the degree of resistance to ion transport through these films was almost same. In general, the coating systems with a resistance greater than 10^8 ohm-cm^2 were categorized as good coatings, while the coating which is less than 10^6 ohm-cm^2 usually showed that the metal underneath the coatings had been attacked and that these Zn·Ph layers have a porous structure which facilitates the penetration of corrosive ions.

Figure 5 shows typical cathodic polarization curves of log current versus potential for Ca-, Cu-, Al-, Co-, and Mn-nitrates-modified Zn·Ph coatings in an aerated 0.5 M NaCl solution. From the comparison of curve features, the current for Mn nitrate-modified coating in the potential region between -0.725 and -0.775 V, was the lowest. The secondary lowest current in the same potential regions was obtained from the Co nitrate-modified coating. In contrast, the other coatings seem to be less effective in shifting current to a lower value. Because a lower current is indicative of a lower hydrogen reaction, the result confirms that the oxygen reduction reaction, $H_2O + 1/2O_2 + 2e^- \rightarrow 2OH^-$, of the steel panel underneath the Zn·Ph layers, was inhibited by incorporating the Co and Mn ions into the Zn·Ph. In fact, the earlier EDX analyses suggested that Co- and Mn-nitrate-modified Zn·Ph layers contain a certain amount of Co and Mn, whereas no metal was found in the Zn·Ph when the other metal nitrates were incorporated in the phosphating solutions. The Al-nitrate compound had the highest current value, corresponding to a high rate of hydrogen reaction; this was due mainly to poor coverage of the steel by discontinuous Zn·Ph layer, so that the metal lacked a barrier against corrosion. The anodic reaction, $Fe^0 - 2e^- \rightarrow Fe^{2+}$, which relates directly to the corrosion of steel, occurs at the Zn·Ph/steel interfaces. The

electrons, $2e^-$, generated by the anodic reaction of Fe in the steel then preferentially reacts with ionic metals with a +2 charge. This reaction can be described as an election trapping reaction [9], M^{2+} (ionic metals) + $2e^-$ = M^0 (elemental metals), and is illustrated schematically as follows.

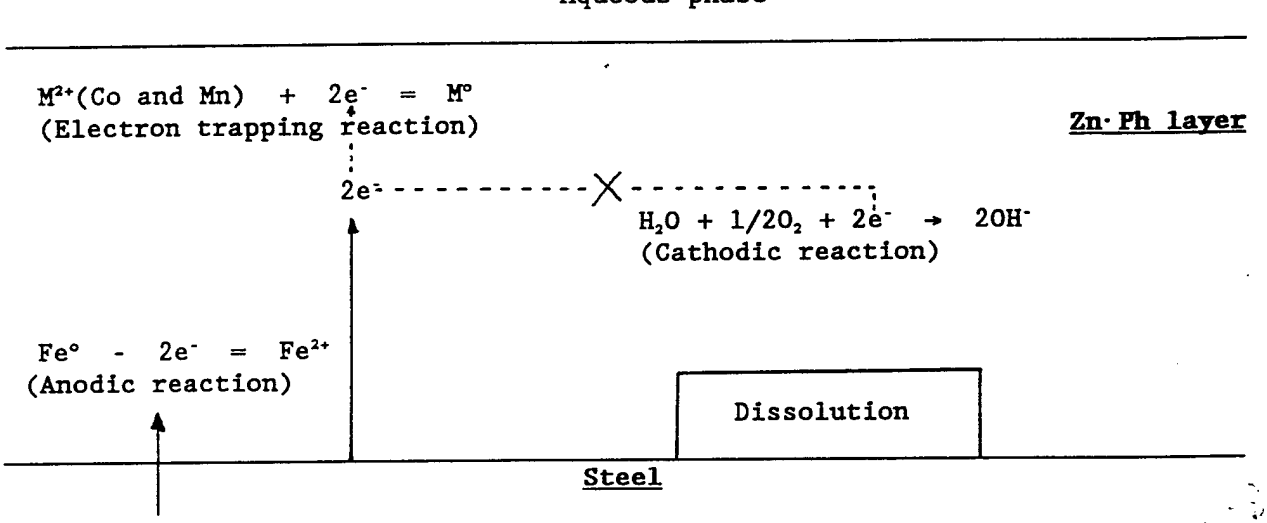

From the viewpoint of the charge balance for the uptake of $2e^-$. the electron trapping behavior of Co^{2+} and Mn^{2+} ions serves to inhibit the cathodic reaction of the steel at corrosion sites. Similarly, the corrosion-inhibiting mechanism of Zn·Ph may reflect the uptake of $2e^-$ by Zn^{2+} ions dissociated from the Zn·Ph. Such a dissociation is caused by the OH^- ions generated by the cathodic reaction inducing the alkali dissolution of Zn·Ph [2]. Hence, incorporating Co^{2+} and Mn^{2+} ions into the Zn·Ph appears to control the alkali dissolution of Zn·Ph, thereby extending the lifetime of the covering which acts as corrosion barrier for the steel.

To support this finding, we further investigated the ability of various metal ions-incorporated Zn·Ph layers to protect the steel against the corrosion. Information on their ability was obtained from the Tafel extrapolation techniques on the potentiodynamic polarization diagrams. Tests were accomplished by exposing Zn·Ph-coated steel panels (surfaces area, 1.0 cm^2) to an aerated 0.5 M sodium

chloride solution at 25°C. Figure 6 shows a typical cathodic-anodic polarization curve which plots the polarization voltage (E) versus current (I) (Tafel plot). Based upon this potentiodynamic polarization curve, we attempted to determine the absolute corrosion rates of Al, expressed in the conventional engineering units of milli-inches per year (mpy). The equation (1) proposed by Sterm and Gery [10] was used in the first step:

$$I_{corr} = \beta_a \cdot \beta_c / 2.303 (\beta_a + \beta_c) R_p \text{ ---------- (1)}$$

where I_{corr} is the corrosion current density in $\mu A/cm^2$, β_a and β_c, having the units of volts/decade of current, refer to the anodic and cathodic Tafel slopes (see Figure 6), respectively, which were obtained from the log I vs E plots encompassing both anodic and cathodic regions, and R_p is the polarization resistance which was determined from the slope of the polarization curve in the potential range of ± 25 mV from the corrosion potential, E_{corr}. When I_{corr} was computed through the equation (1), the corrosion rate (mpy) can be obtained from the following expression (2):

$$\text{Corrosion rate} = 0.13\ I_{corr}\ (EW) / d \text{ ----------(2)}$$

where EW is the equivalent weight of the corroding species in g, and d is the density of the corroding species in g/cm^3.

Table 4 gives the I_{corr} and corrosion rate for Zn·Ph panels treated with various metal nitrates. These data are the average of three panels. The averaged corrosion rate of the bare 1008 steel panel was 20.7 mpy, corresponding to the averaged I_{corr} of 45.2 $\mu A/cm^2$. The corrosion rate of bare panel was significantly reduced by depositing Zn·Ph layers derived from the Ca-, Mg-, Cu-, Fe-, Co-, and Mn-nitrates-incorporated phosphating solutions onto the panel's surfaces. In particular, the rates for the Co- and Mn-nitrates panels were lower than those of other Zn·Ph panels. As expected, a high rate of corrosion can be seen from the Al nitrate-related Zn·Ph layer, reflecting a poor coverage of panel's surfaces by a discontinuous layer. Thus, we believe that the electron trapping behaviors of Co^{2+} and Mn^{2+} inhibit the corrosion of the panels.

This information was correlated directly with the changes in salt-spray resistance of these Zn·Ph panels as a function of Fe^{2+} ions. The data (Table 5) verified that a high concentration of Fe^{2+} ions in the phosphating solution for all Zn·Ph panels confers extended protection against NaCl-related corrosion. The most effective metal nitrate was $Mn(NO_3)_2 \cdot 6H_2O$, with the $Co(NO_3)_2 \cdot 6H_2O$ as the second most effective one. The Mn nitrate-Zn·Ph coatings prepared in

concentrations of Fe^{2+} ion ranging from 0.56 to 0.78 % displayed the resistance to salt spray for 120 hrs. Increasing the concentration of Fe^{2+} ions to 0.88 led to an excellent performance, reflecting a salt-spray resistance of 144 hrs. Although Fe^{2+} ions of > 0.8 % were incorporated into the phosphating solution containing other nitrates, no significant protection was given by these Zn·Ph coatings; their maximum resistance in the salt-spray chamber was only 48 hrs. Consequently, we believe that the $Mn(NO_3)_2 \cdot 6H_2O$ has a high potential for replacing $Co(NO_3)_2 \cdot 6H_2O$ which is known to be an environmentally hazardous material. The major assignments of the Mn nitrate additive in fabricating a high quality Zn·Ph coating are as follows; when this additive comes in contact with the phosphating solution, the ionic nitrate species creates a large number of crystal nucleate sites on the steel panel's surfaces, thereby resulting in a good coverage of the surfaces by a continuous layer of Zn·Ph. Furthermore, the Mn^{2+} ions incorporated into the Zn·Ph acted to inhibit the cathodic reaction in terms of the oxygen reduction reaction, $H_2O + 1/2O_2 + 2e^- \rightarrow 2OH^-$, of the steel because of the uptake of $2e^-$ generated from the anodic reaction, $Fe^0 - 2e^- \rightarrow Fe^{2+}$, which occurs at the corrosion sites of steel, by the Mn^{2+} ions. Inhibiting the cathodic reaction by the electron trapping behavior of Mn^{2+}, $Mn^{2+} + 2e^- = Mn^0$, not only reduced the rate of corrosion, but also contributed to extending lifetime of Zn·Ph as the corrosion barrier.

3.3 Polyelectrolyte Rinsing

The goal of this part of the research was to gain technical information on the poly(acrylic acid) [p(AA)] polyelectrolyte solutions used to replace the conventional Cr-based rinsing solution. This involved determining an optimum concentration of p(AA) to improve further the protective ability of Zn·Ph coatings, and also assessing the important of the drying temperature of p(AA) solution-rinsed Zn·Ph coatings, prepared from phosphating solutions containing various concentration of free Fe^{2+} ions, in improving salt-spray resistance. In this work, all the Zn·Ph coatings were made from a 1 wt% $Mn(NO_3)_2 \cdot 6H_2O$-modified phosphating solution at 80°C. The concentrations of p(AA) solid dissolved in an aqueous solution ranged from 0.00 to 6.25 wt%. As is evident from its wide application in cleaners, binders, emulsion paints, dental cements, and synthetic cooling waters, the hazard rating of p(AA) solution is moderate [11, 12]. The Zn·Ph-coated panels were dipped into the p(AA) solution for a few seconds at 25°C

to rinse them, and then the p(AA)-wetted panels were dried in an oven at temperatures up to 150°C for 20 min.

Table 6 shows the results of salt-spray resistance tests for Zn·Ph panels rinsed with 0, 1.25, 2.5, 3.75, 5.0, and 6.25 wt% p(AA) solutions as a function of concentration of Fe^{2+} ions incorporated in the phosphating solution. The p(AA)-rinsed panels were dried in an oven at 150°C for 20 min. The results show that salt-spray resistance is significantly improved by rinsing the panels with p(AA) solutions. For instance, a resistance of 144 hrs for Zn·Ph panels derived from 0.9 % Fe^{2+} ion-incorporated phosphating solution was improved to 480 hrs when they were rinsed with only 1.25 % p(AA). As expected, an increase in the concentration of p(AA) further improved resistance. However, there was no significant effect on extension of this resistance by adding p(AA) > 3.75 %. A resistance of 1008 hrs obtained from a 3.75 % p(AA)-rinsed Zn·Ph coating with 0.90 % Fe^{2+} ions corresponded to a striking increase in seven fold over that of no-rinsed Zn·Ph coatings made from the same concentration of Fe^{2+} ions. Moreover, the increase in resistance also appears to depend on the concentration of Fe^{2+} ions added to the phosphating solution; a high concentration of Fe^{2+} contributed to better protection than that of a low Fe^{2+} content. For instance, using the 3.75 % p(AA), the resistance of Zn·Ph coatings made from 0.90 % Fe^{2+} was considerably higher (1008 vs 480 hrs) than that from 0.33 % Fe^{2+}. Nevertheless, a 3.75 % seems to be an appropriate concentration of p(AA) for using as rinsing solution.

Next, our attention centered upon determining an optimum temperature for drying the p(AA)-wetted Zn·Ph surfaces. Two formulations of the phosphating solutions containing 0.50 and 0.63 % Fe^{2+} were adopted to prepare the Zn·Ph test panels. After dipping the panels in a 3.75 % p(AA) solution, they were left for 20 min in an oven at 75, 100, 125, or 150°C. The results from the salt-spray resistance testings for these panels are shown in Table 7. The data verified that even though the panels were dried at low temperature of 75°C, the extent of resistance is almost the same as that of 150°C-dried panels. Thus, we decided that a good way to dry the p(AA)-wetted Zn·Ph panels is to leave them for 20 min in an oven around 80°C.

3.4 Affinity of p(AA)-Rinsed Zn·Ph Surfaces with Electrically Deposited Polymer Topcoatings

To investigate the electrochemical attraction of p(AA) electrolyte polymer layers existing at the outermost surface sites of Zn·Ph layers to the polyurethan-modified epoxy polymer topcoating (POWERCRON 648), we studied the changes in three parameters, voltage, bath temperature and operating time, on the electric deposition technology employed for fabricating the topcoat onto the Zn·Ph surfaces, as a function of concentration of p(AA). After depositing, the polymeric films were cured by leaving them for 30 min in an oven at 177°C. The average thickness of film built up on the Zn·Ph surface was ≈ 1.0 mil. In this test, the Zn·Ph panels rinsed with 0, 1.25, 2.5, 3.75, and 5.0 wt% p(AA) solutions. The results from these specimens are shown in Table 8. The data demonstrated that an increase in the concentration of p(AA) reduces the time taken for depositing this polymer at a low voltage and bath temperature. This finding suggests that the p(AA) has a strong electrochemical affinity with the POWERCRON 648 topcoating in the electodeposition bath, thereby introducing excellent interfacial bonds at interfaces between them.

4. Conclusions

We draw the following conclusions from the information described above. The metal nitrate hydrate compounds, especially $Mn(NO_3)_2 \cdot 6H_2O$ and $Co(NO_3)_2 \cdot 6H_2O$ employed as additives to the zinc phosphating solutions, played two important roles in forming good crystalline zinc phosphate (Zn·Ph) conversion coatings which protect cold-rolled steels against corrosion. One was to create many nucleate sites of embryonic Zn·Ph crystals, thereby ensuring a complete coverage of the steel surfaces by a void-free continuous Zn·Ph layer. The other role was to reduce the rate of the oxygen reduction reaction, $H_2O + 1/2O_2 + 2e^- \rightarrow 2OH^-$, occurring at the cathodic corrosion sites of steel underneath the Zn·Ph layers. The former role was due to the ionic nitrate species dissociated from the metal nitrate compounds in the aqueous medium, and the latter one reflected the uptake of electrons, $2e^-$, generated by the anodic corrosion reaction of Fe in the steel, by Co^{2+} and Mn^{2+} ions liberated from the nitrate compounds. Such electron trapping behavior of these metal ions not only inhibits corrosion, but also significantly contributes to the extended service-life of the Zn·Ph layers because of a decrease in the extent of their susceptibility to alkali dissolution in a high pH environment generated by the oxygen reduction reaction. Moreover, our findings suggested that $Mn(NO_3)_2 \cdot 6H_2O$ additive can substitute for the environmentally

regulated Co- and Ni-nitrate compounds. Once the nucleate sites of embryonic crystals were developed by ionic nitrate species, the rate of crystal growth depended on the concentration of ferrous (II) ions in the phosphating solution; namely, a high concentration of Fe^{2+} ions isolated from the $FeSO_4 \cdot 7H_2O$ used as the source of ferrous ions promoted the rate of crystal growth. We found that incorporating at least 0.52 % Fe^{2+} ions into the solution was required to quickly achieve a reasonable coverage of steel surface by Zn·Ph.

Cr-containing compounds known to be environmental hazards are commonly applied in rinsing Zn·Ph layer surfaces because they improve the ability of Zn·Ph to protect steel from corrosion. Hence, our attention was paid to find the replacing materials for the Cr-related compounds in the rinsing solutions. We demonstrated that the environmentally acceptable poly(acrylic acid) [p(AA)], which is one of the anionic polyelectrolyte family, had a high potential as a replacing material. In fact, Zn·Ph-coated steels rinsed with a 3.75 % p(AA)-dissolved aqueous solution displayed excellent salt-spray resistance for 1008 hrs, corresponding to a seven-fold improvement over that of Zn·Ph specimens that were not rinsed. In addition, p(AA) film existing at outermost surface sites of Zn·Ph layers had a strong electrochemical affinity with the polyurethane-modified epoxy topcoating induced by the electrodeposition technology; hence, only a low voltage and bath temperature were needed to adhere the polymeric topcoat to the p(AA)-rinsed Zn·Ph coatings in a short electrodepositing time. Such affinity at the critical boundary zones might lead to the development of strong interfacial bonds at interfaces between the p(AA) and topcoats.

5. Recommendations

The following four descriptions from the integration of our work performed in FY 94 as Phase I research, can be illustrated in recommendations given below.

1. The optimum formulation for a zinc phosphating solution suitable for 1008 cold-rolled steels was 5 wt% $Zn_3(PO_4)_2 \cdot 2H_2O$ powder, 10 wt% (85 % H_3PO_4), and 85 wt% water, in conjunction with $Mn(NO_3)_2 \cdot 6H_2O$ and $FeSO_4 \cdot 7H_2O$ additives of 1.0 % and 3.0 % by total weight of basic zinc phosphating solutions, respectively.

2. Using the process technology developed in this work, the zinc phosphate

(Zn·Ph) conversion coatings were prepared in accordance with the following sequence: 1) immersing the surface-cleaned steel substrates for 30 min into the phosphating solution at 80°C, 2) rinsing the Zn·Ph-coated steel surfaces with water, 3) dipping the water-rinsed Zn·Ph coating specimens for few seconds into a 3.75 wt% p(AA) aqueous solution, and 4) drying the p(AA)-wetted Zn·Ph coating specimens for 20 min in an oven at 80°C.

3. To complete our investigation of the biodegradable enzymatic cleaning solutions which will prevent the formation of excessive oxides or hydroxides on the steel surfaces, continuation of this work will be needed in the next fiscal year.

4. Although Zn·Ph coatings are responsible for improving corrosion resistance in vehicles by delaying the onset of "red rust" of various discrete parts, such as fasteners and brackets, it is commonly known that in the automotive industry electrogalvanized coatings (EGCs) currently have the major share of the auto-motive body-panel market. However, there are two problems in using EGCs. One is the poor adherence of galvanized (zinc) coating surfaces to the polymeric topcoats, and the other is the necessity of post-treatment to inhibit the onset of "white rust", which represents deterioration of the zinc layer. The surface modification of EGCs by Zn·Ph coatings is very attractive as one way to solve these problems. Thus, the development of zinc phosphating solutions compatible with EGCs will be needed.

6. Acknowledgments

The authors are grateful to Dr. Robert R. Reeber, U.S. Army Research Office (ARO), for his invaluable suggestions; and to Dr. Joseph Lucas, PPG Industries, Inc., for his assistance to prepare electrodeposited topcoatings on the Zn·Ph surfaces. Discussions with Mr. Willem J. Steyn, RHO Technologies Inc., and Mr. Philip H. Austin, The Palnut Company, are also appreciated

References

1. T. Sugama, L.E. Kukacka, N. Carciello, and J.B. Warren, J. Materials Science, 23, 101 (1988).
2. T. Sugama, L.E. Kukacka, and N. Carciello, J. Coatings Tech. 61, 43 (1989).
3. T. Sugama, and J.K. Pak, Adv. Materials & Manufacturing Processes, 6, 227 (1991).
4. T. Sugama, and R. Broyer, Surface & Coatings Technology, 50, 89 (1992).
5. T. Sugama, and N. Carciello, J. Appl. Poly. Science, 50, 1701 (1993).
6. T. Sugama, and T. Takahashi, J. Materials Science, 30, 809 (1995).
7. W.J. Loreny, and F. Mansfield, Corr. Sci., 21, 647 (1981).
8. F. Mansfield, M.W. Kending, and S. Tsai, Corrosion, 38, 478 (1982).
9. H. Leidheiser, Jr., and I. Suzuki, J. Electrochem. Soc., 128, 241 (1981).
10. M. Sterm, and A. Geary, J. Electochem. Soc., 104, 56 (1957).
11. W.M. Hann, S.T. Robertson, and J.H. Bardsley, "Recent Experience in Controlling Silica and Magnesium Silicate Deposits with Polymeric Dispersant" Fifty-Fourth Annual International Water Conference, Pittsburgh, PA, October 11-13, 1993.
12. W.M. Hann, J.H. Bardsley, and S.T. Robertson, "ACUMER Water Treatment Polymers" Technical Report, Rohm and Haas Company, 1995.

Table 1. Effect of Fe^{2+} Ions Dissociated from $FeSO_4 \cdot 7H_2O$ in the Phosphating Solution on the Coverage of Panel Surfaces by Zn·Ph Crystals

Concentration of Fe^{2+} ion, %	Coverage	Salt-spray resistance, hr
0.00	None	1
0.15	None	1
0.26	Poor	10
0.37	Poor	24
0.52	Good	72
0.62	Good	72
0.76	Good	72
0.86	Good	82
0.90	Good	82
1.00	Good	82

Table 2 Salt-Spray Resistance of Zn·Ph Coatings Derived from $Co(NO_3)_2 \cdot 6H_2O$-Modified and Unmodified Phosphating Solution as a Function of Concentration of Fe^{2+} Ions

Phosphating solution	Concentration of Fe^{2+} ion, %	Salt-spray resistance, hr
Unmodified	0.44	1
Unmodified	0.61	10
Unmodified	0.79	10
Unmodified	0.99	24
Unmodified	1.10	24
$Co(NO_3)_2 \cdot 6H_2O$-modified	0.37	24
$Co(NO_3)_2 \cdot 6H_2O$-modified	0.62	72
$Co(NO_3)_2 \cdot 6H_2O$-modified	0.76	72
$Co(NO_3)_2 \cdot 6H_2O$-modified	0.90	82
$Co(NO_3)_2 \cdot 6H_2O$-modified	1.00	82

Table 3. Comparison Between Impedance Values of Conversion Coatings Derived from Various Metal Nitrates-Modified Phosphating Solutions.

Metal nitrate compound	Impedance at 0.5 Hz, $\|Z\|$, ohm-cm^2
$Ca(NO_3)_2 \cdot 4H_2O$	4.0×10^2
$Mg(NO_3)_2 \cdot 6H_2O$	4.2×10^2
$Cu(NO_3)_2 \cdot 3H_2O$	4.0×10^2
$Fe(NO_3)_3 \cdot 9H_2O$	4.1×10^2
$Al(NO_3)_3 \cdot 9H_2O$	2.6×10^2
$Co(NO_3)_2 \cdot 6H_2O$	4.5×10^2
$Mn(NO_3)_2 \cdot 6H_2O$	4.8×10^2

Table 4. I_{corr} and Corrosion Rate Obtained from Tafel Calculation for Zn·Ph Panels Derived from Various Metal Nitrates-Modified Phosphating Solutions.

Metal nitrate compound	I_{corr}, $\mu A/cm^2$	Corrosion rate, mpy
Control (bare 1008 steel)	45.2	20.7
$Ca(NO_3)_2 \cdot 4H_2O$	1I.5	5.3
$Mg(NO_3)_2 \cdot 6H_2O$	12.6	5.8
$Cu(NO_3)_2 \cdot 3H_2O$	13.9	6.4
$Fe(NO_3)_3 \cdot 9H_2O$	12.3	5.6
$Al(NO_3)_3 \cdot 9H_2O$	24.1	11.0
$Co(NO_3)_2 \cdot 6H_2O$	10.9	4.5
$Mn(NO_3)_2 \cdot 6H_2O$	9.6	4.3

Table 5. Salt-Spray Resistance of Zn·Ph Conversion Coatings Derived from Various Metal Nitrates (1wt%)-Modified Phosphating Solutions.

Metal nitrate compound	Free Fe^{2+} ion, %	Salt-spray resistance hrs
$Co(NO_3)_2 \cdot 6H_2O$	0.37	24
$Co(NO_3)_2 \cdot 6H_2O$	0.52	72
$Co(NO_3)_2 \cdot 6H_2O$	0.62	72
$Co(NO_3)_2 \cdot 6H_2O$	0.76	72
$Co(NO_3)_2 \cdot 6H_2O$	0.86	82
$Co(NO_3)_2 \cdot 6H_2O$	0.90	82
$Co(NO_3)_2 \cdot 6H_2O$	1.00	82
$Fe(NO_3)_3 \cdot 9H_2O$	0.48	24
$Fe(NO_3)_3 \cdot 9H_2O$	0.57	24
$Fe(NO_3)_3 \cdot 9H_2O$	0.63	24
$Fe(NO_3)_3 \cdot 9H_2O$	0.76	48
$Fe(NO_3)_3 \cdot 9H_2O$	0.86	48
$Ca(NO_3)_2 \cdot 4H_2O$	0.35	24
$Ca(NO_3)_2 \cdot 4H_2O$	0.43	24
$Ca(NO_3)_2 \cdot 4H_2O$	0.56	48
$Ca(NO_3)_2 \cdot 4H_2O$	0.62	48
$Ca(NO_3)_2 \cdot 4H_2O$	0.71	48
$Ca(NO_3)_2 \cdot 4H_2O$	0.86	48
$Mg(NO_3)_2 \cdot 6H_2O$	0.34	24
$Mg(NO_3)_2 \cdot 6H_2O$	0.53	24
$Mg(NO_3)_2 \cdot 6H_2O$	0.60	48
$Mg(NO_3)_2 \cdot 6H_2O$	0.75	48
$Mg(NO_3)_2 \cdot 6H_2O$	0.89	48
$Cu(NO_3)_2 \cdot 3H_2O$	0.33	24
$Cu(NO_3)_2 \cdot 3H_2O$	0.56	24
$Cu(NO_3)_2 \cdot 3H_2O$	0.63	48
$Cu(NO_3)_2 \cdot 3H_2O$	0.72	48
$Cu(NO_3)_2 \cdot 3H_2O$	0.89	48
$Cu(NO_3)_2 \cdot 3H_2O$	0.94	48
$Mn(NO_3)_2 \cdot 6H_2O$	0.24	48
$Mn(NO_3)_2 \cdot 6H_2O$	0.37	72
$Mn(NO_3)_2 \cdot 6H_2O$	0.46	96
$Mn(NO_3)_2 \cdot 6H_2O$	0.56	120
$Mn(NO_3)_2 \cdot 6H_2O$	0.63	120
$Mn(NO_3)_2 \cdot 6H_2O$	0.78	120
$Mn(NO_3)_2 \cdot 6H_2O$	0.88	144
$Al(NO_3)_3 \cdot 9H_2O$	0.60	10
$Al(NO_3)_3 \cdot 9H_2O$	0.78	10
$Al(NO_3)_3 \cdot 9H_2O$	0.90	24
$Al(NO_3)_3 \cdot 9H_2O$	1.10	24

Table 6. Changes in Salt-Spray Resistance of Conversion Coatings After Rinsing with Aqueous Solutions Containing p(AA) of Various Concentrations as a Function of Fe^{2+} Ions.

Concentration	Salt-spray resistance, hrs					
of Fe^{2+}, %	0.0%p(AA)	1.25%p(AA)	2.5%p(AA)	3.75%p(AA)	5.0%p(AA)	6.23%p(AA)
0.33	72	144	168	480	500	504
0.49	96	168	336	576	528	528
0.63	120	312	576	684	624	528
0.79	120	336	840	888	816	528
0.90	144	408	984	1008	816	528

Table 7. Salt-Spray Resistance for 3.75 % p(AA)-Rinsed Zn·Ph Coatings After Drying for 20 min at Temperatures up to 150°C.

Concentration of	Salt-spray resistance, hrs			
Fe^{2+} ion, %	75°C	100°C	125°C	150°C
0.50	580	576	530	576
0.63	648	670	648	684

Table 8. Changes in Electrodeposition Parameters, Voltage, Bath Temperature, and Operating Time, as Function of Concentration of p(AA).

Concentration of p(AA), wt%	Voltage, V	Temperature, °C	Time, Sec.
0.00	225	32	120
1.25	225	32	120
2.50	175	32	120
3.75	100	29	100
5.00	100	27	90

LEGENDS FOR FIGURES

Figure 1. SEM images coupled with EDX spectra for Zn·Ph conversion coatings derived from $Ca(NO_3)_2 \cdot 4H_2O$ (top)- and $Cu(NO_3)_2 \cdot 3H_2O$ (bottom)-modified zinc phosphating solutions.

Figure 2. SEM-EDX images of conversion coatings derived from $Al(NO_3)_3 \cdot 9H_2O$ (top)- and $Fe(NO_3)_3 \cdot 9H_2O$ (bottom)-modified phosphating solutions.

Figure 3. SEM-EDX data for conversion coatings derived from $Co(NO_3)_2 \cdot 6H_2O$ (top)- and $Mn(NO_3)_2 \cdot 6H_2O$ (bottom)-incorporated phosphating solutions.

Figure 4. Bode plots for bare steel substrate and Zn·Ph-coated steel specimens.

Figure 5. Comparisons of cathodic polarization curves for conversion coatings derived from various metal nitrates-modified phosphating solutions.

Figure 6. Typical Tafel plot from a polarization experiment.

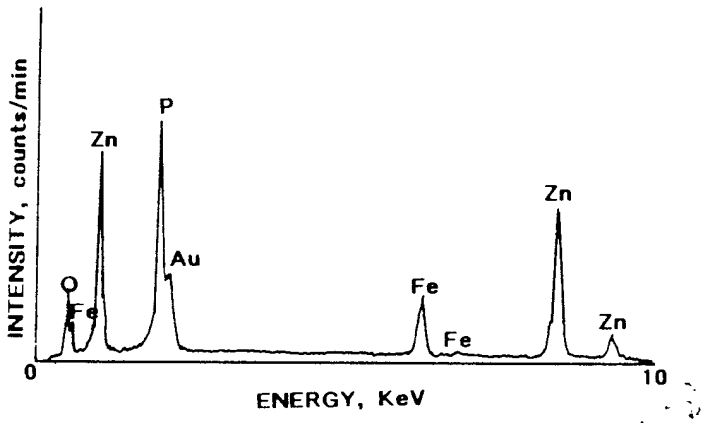

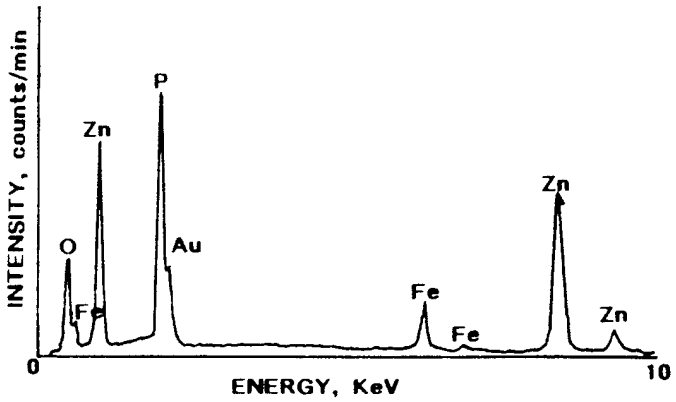

Figure 1. SEM images coupled with EDX spectra for Zn·Ph conversion coatings derived from $Ca(NO_3)_2 \cdot 4H_2O$ (top)- and $Cu(NO_3)_2 \cdot 3H_2O$ (bottom)-modified zinc phosphating solutions.

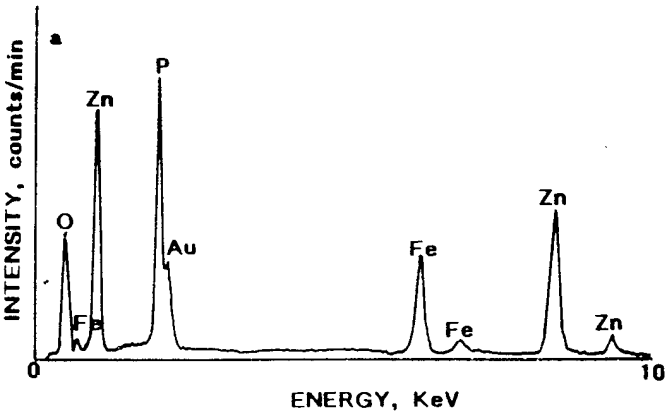

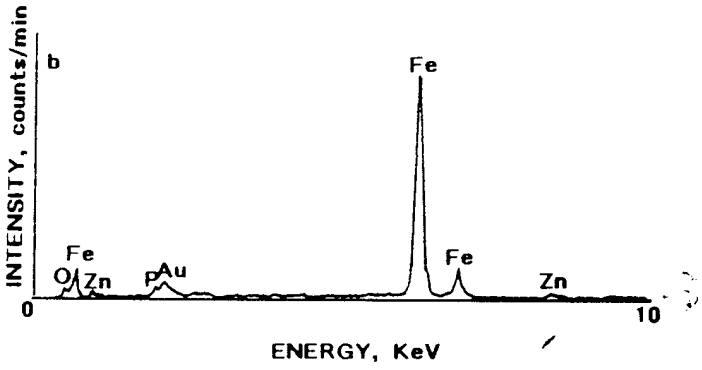

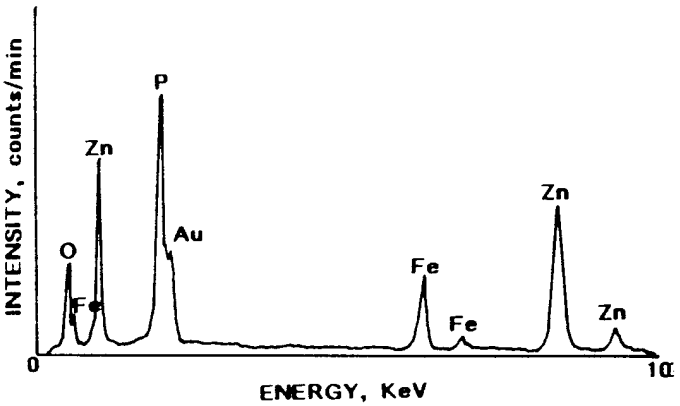

Figure 2. SEM-EDX images of conversion coatings derived from $Al(NO_3)_3 \cdot 9H_2O$ (top)- and $Fe(NO_3)_3 \cdot 9H_2O$ (bottom)-modified phosphating solutions.

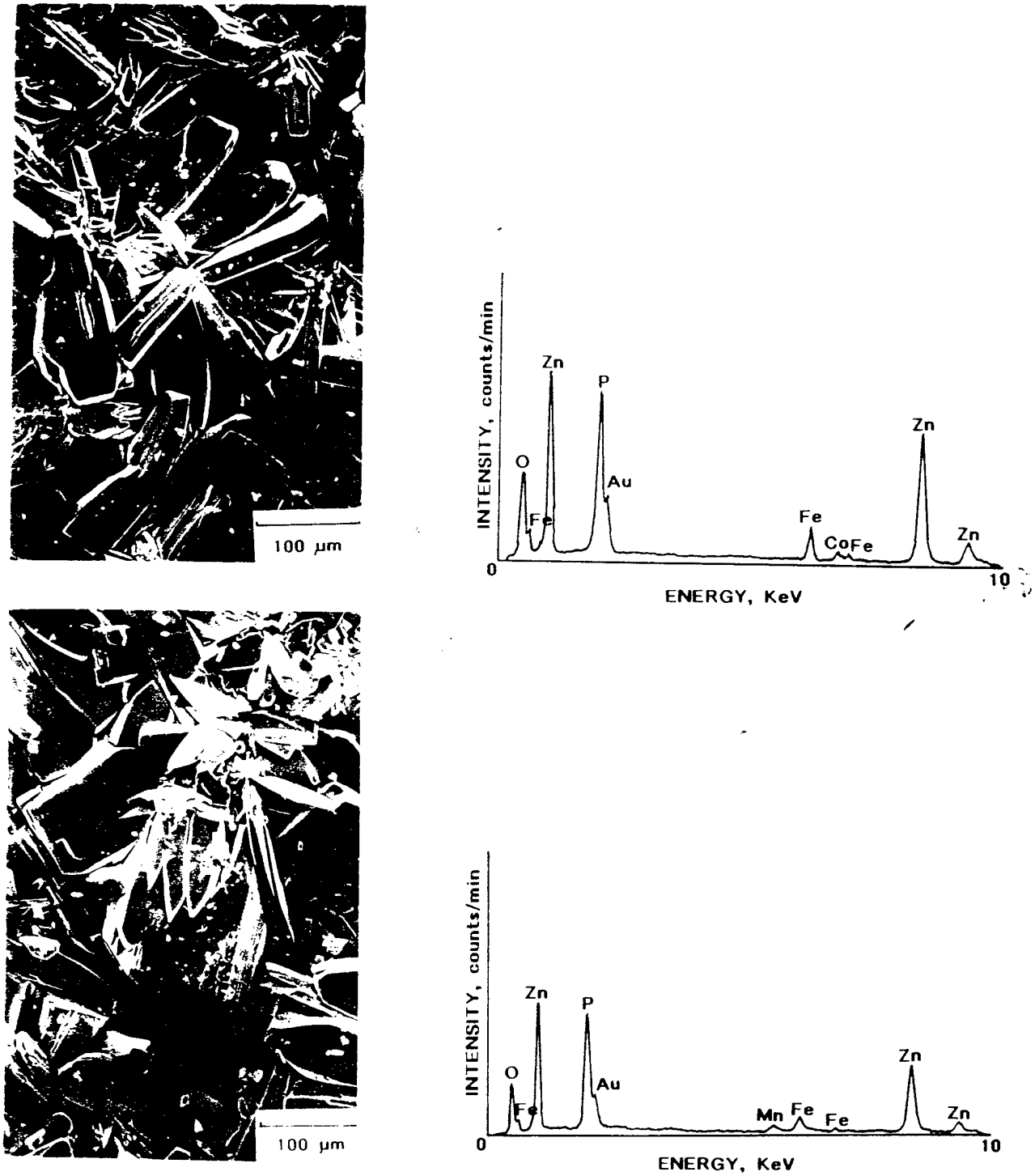

Figure 3. SEM-EDX data for conversion coatings derived from $Co(NO_3)_2 \cdot 6H_2O$ (top)- and $Mn(NO_3)_2 \cdot 6H_2O$ (bottom)-incorporated phosphating solutions.

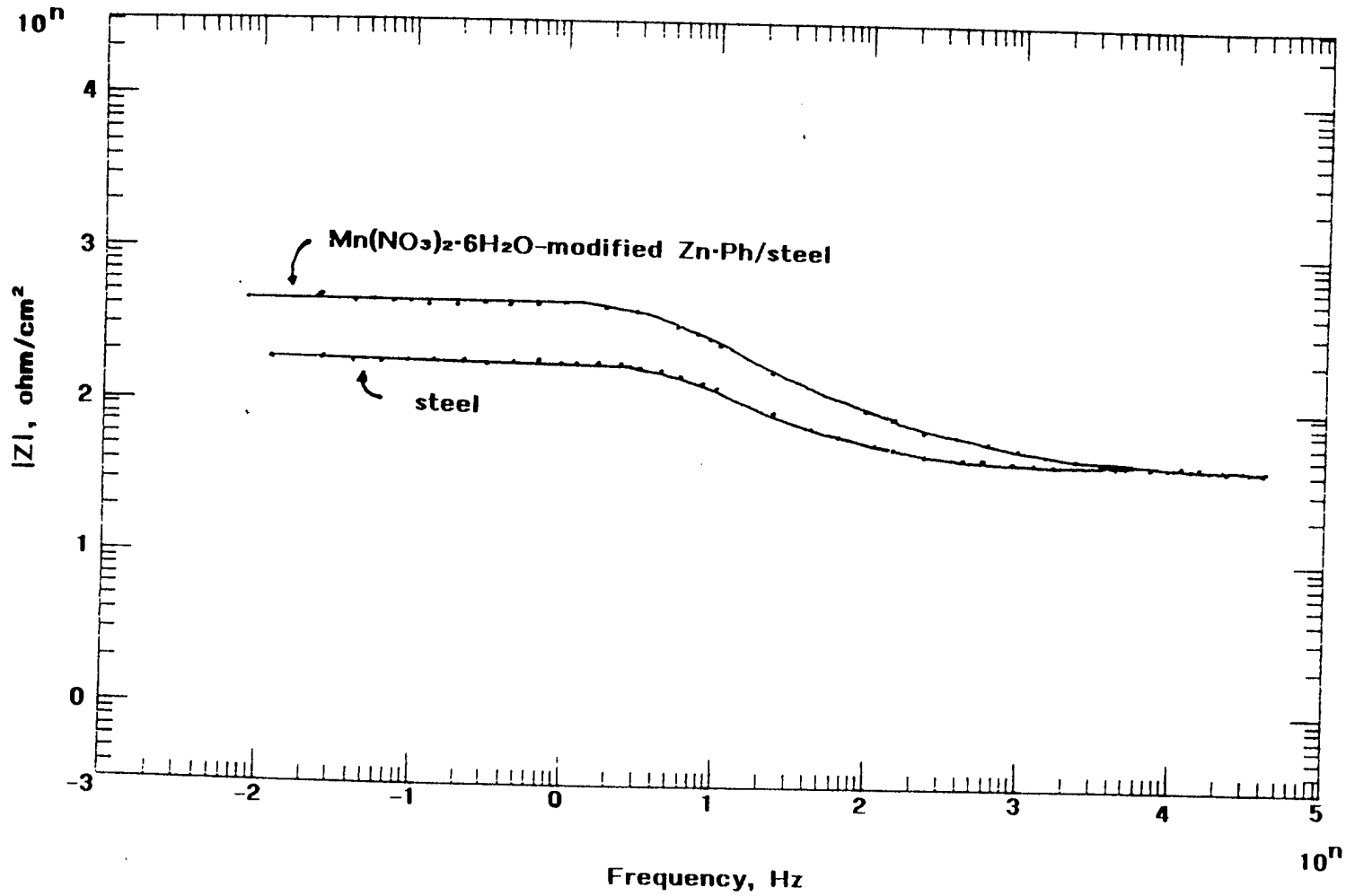

Figure 4. Bode plots for bare steel substrate and Zn·Ph-coated steel specimens.

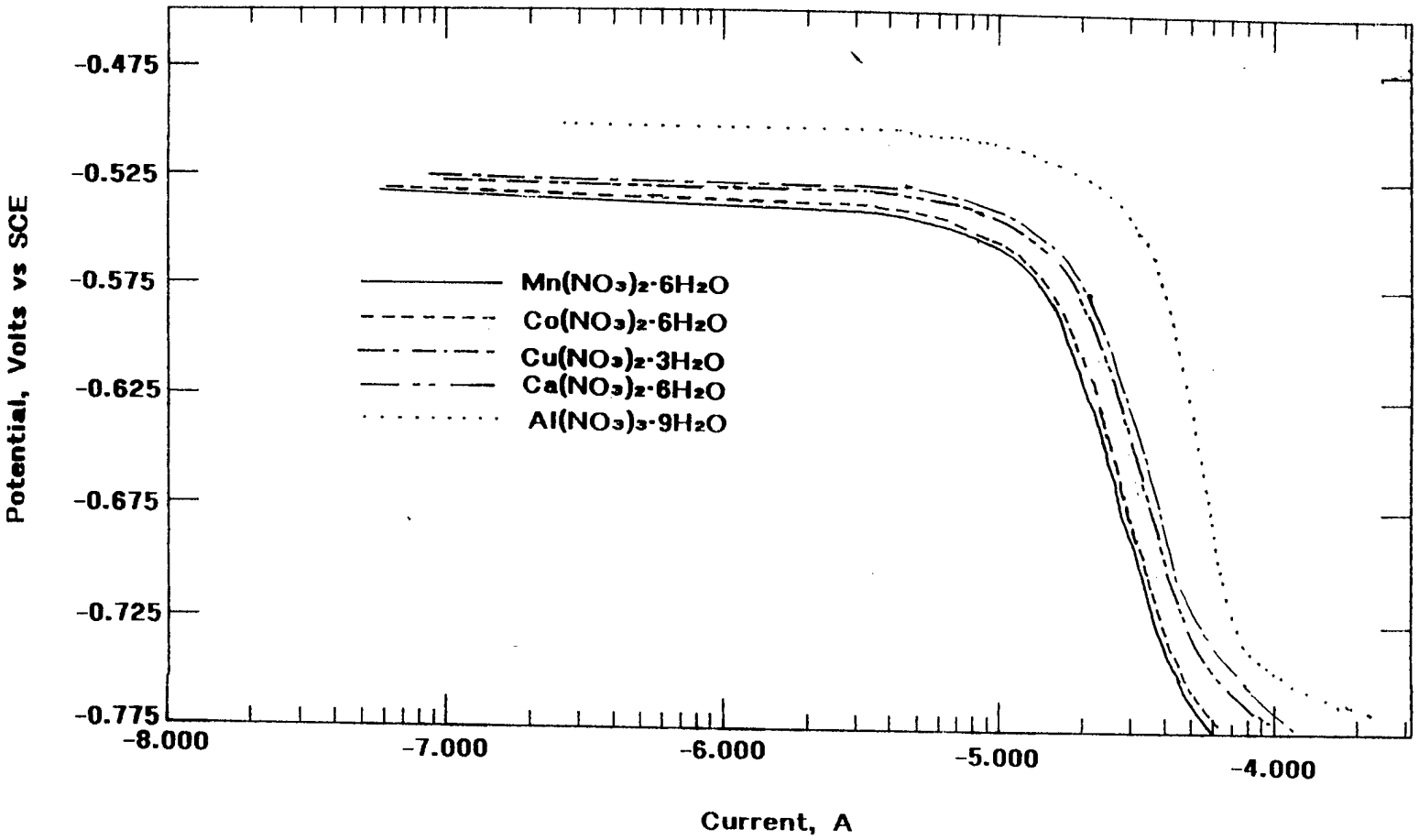

Figure 5. Comparisons of cathodic polarization curves for conversion coatings derived from various metal nitrates-modified phosphating solutions.

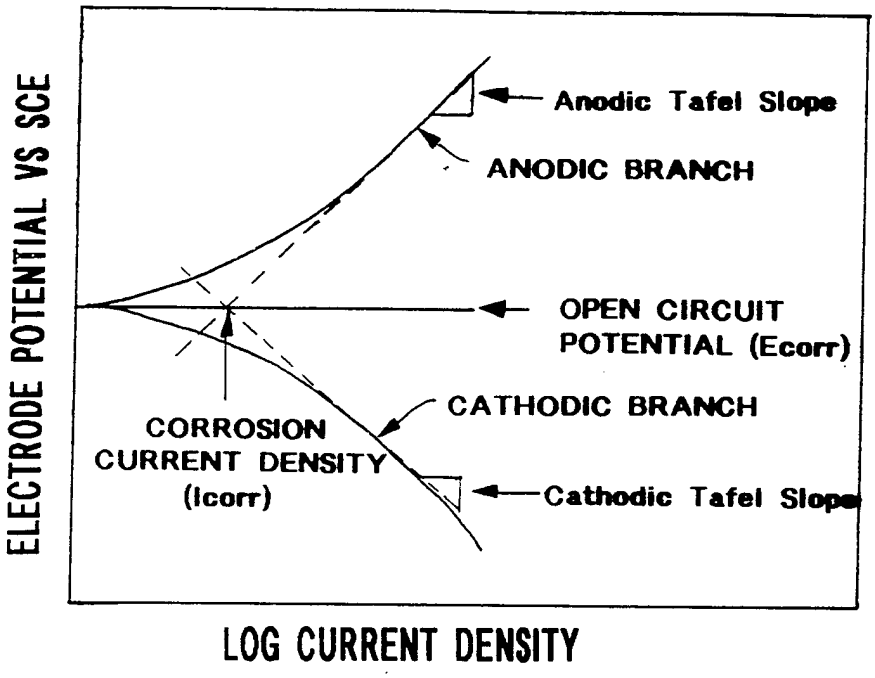

Figure 6. Typical Tafel plot from a polarization experiment.